THERMODYNAMIC ANALYSIS AND OPTIMIZATION OF A JET EJECTOR REFRIGERATION CYCLE USED TO COOL DOWN THE INTAKE AIR IN AN IC ENGINE

J. Galindo, V. Dolz[1], A. Tiseira, A. Ponce-Mora

CMT – Motores Térmicos, Universitat Politècnica de València, Spain

Abstract

The present paper evaluates a jet ejector refrigeration system intended to cool down diesel engine intake below ambient conditions. Performance is assessed by means of 1D thermodynamic model of the cycle fed with ejector maps obtained with CFD code using R134a as working fluid. In the first study, no particular ejector geometry is fixed thus allowing the genetic algorithm to adapt the cycle to different engine conditions. Following this approach engine intake temperatures close to 0 $°C$ can be attained in those engine operating points in which exhaust thermal power is sufficient to drive the jet-ejector refrigeration system. In the second evaluation, ejection cycle configuration which provided best results for the most frequent operating point in a standard driving, designated as 2000 rpm and 50% load, is selected. With this particular configuration the rest of engine operating points are reassessed. In this study performance degradation is found away from the design point showing that ejector size is a limiting factor.

Keywords

Waste heat recovery, jet ejector refrigeration cycle, internal combustion engine, performance optimization, genetic algorithm

NOMENCLATURE

Acronyms

COP	Coefficient Of Performance
EGR	Exhaust Gas Recirculation
GWP	Global Warming Potential
ICE	Internal Combustion Engine
ODP	Ozone Depletion Potential
ORC	Organic Rankine Cycle
WHR	Waste Heat Recovery

Notation

Latin

[1] Corresponding Author: Vicente Dolz, CMT – Motores Térmicos, Universitat Politècnica de València, 46022, Spain. Email: vidolrui@mot.upv.es

A	Area (m^2)
c	Specific Heat Capacity (J kg^{-1} K^{-1})
d	Diameter (mm)
h	Specific enthalpy (J kg^{-1})
k	Pump pressure ratio (-)
$\dot{m}$	Mass flow rate (kg s^{-1})
P	Pressure (bar)
$\dot{Q}$	Heat Exchanger Power (W)
R	Gas constant (J kg^{-1} K^{-1})
s	Specific entropy (J kg^{-1} K^{-1})
T	Temperature (°C)
x	Vapor quality (-)
Z	Compressibility factor (-)

Greek letters

α	Curve fit coefficient (-)
β	Ejector scaling factor (-)
η	Isentropic efficiency (-)
π	Ejector pressure ratio (-)
ω	Ejector entrainment ratio (-)

Subscripts

$1-9$	Cycle state points
$1f-6f$	Curve fit coefficient index
co	Condenser
$crit$	Ejector critical operating mode
ev	Evaporator
ex	ICE exhaust
ge	Generator
i	Inlet
in	ICE intake
m	Ejector mixing chamber
n	Ejector primary nozzle
o	Outlet
pr	Primary flow
pm	Pump
sec	Secondary flow
s	Isentropic conditions
sat	Saturated conditions
$scrit$	Ejector subcritical operating mode
sm	Numerically simulated
sup	Superheating
t	Ejector primary nozzle throat
$total$	Sum of condenser, evaporator and generator
v	Vapor state
vl	Expansion valve
w	Condenser water

1. Introduction

The growing concern about environmental impact of human activity has led to the development of different technologies which support a more efficient use of available resources. Low-grade waste heat coming from industrial processes, solar energy, or thermal engines exhaust offers potential to be reused, thus contributing to significant energy savings. Applicability range of this energy is vast and particular application of generating a cooling capacity by means of ejection cycles has a great potential. Air conditioning and food preservation are promising application areas owing to their widespread use and their significant power consumption (Diaconu, 2012; Guo and Shen, 2009; Tassou et al., 2010). A significant part of recent developments in ejector refrigeration technologies in the aforementioned areas are focused on energy-efficient alternatives to the traditional systems, with special interest in systems using carbon dioxide (R744) as a refrigerant (Gullo et al., 2017; Hafner and Banasiak, 2016).

Despite its reduced energy input to drive the system (mainly due to liquid pump) and simplicity with respect to traditional air conditioning systems ejection cycles driven by waste heat have not been widely adopted due to their relatively low COP and performance degradation away from design conditions.

In the internal combustion engines research field, ejection cycles and ejector technology implementation show potential benefits when applied both raising conventional air conditioning performance and generating a cooling capacity by means of exhaust energy. The first concept was developed and implemented in a vehicle by the Japanese company Denso. During the last years several designs have been patented by this company using different approaches with jet ejector technology (Takeuchi, 2011a, 2011b) and some of them have been implemented in passenger vehicles and trucks. The second approach is framed within different strategies of waste heat recovery (WHR) and it is focused on an exhaust heat driven cooling system. In an internal combustion engine for automotive applications approximately one third of available fuel energy is lost as exhaust waste heat and an additional one third is lost by the cooling water so the implementation of these systems could lead to a significant efficiency improvement. Several approaches have been under investigation to unlock this potential: absorption refrigeration units (Koehler et al., 1997; Manzela et al., 2010; Talom and Beyene, 2009), adsorption refrigeration systems (Jiangzhou et al., 2003; Meunier, 2001; Zhang, 2000), ejector refrigeration systems (Zegenhagen and Ziegler, 2015a, 2015b) or hybrid ejector and vapor compression systems (X. Chen et al., 2013).

Some WHR technologies like ORC or thermoelectric generators produce direct benefits which are measurable in terms of shaft power or electric power. In the case of WHR technologies intended for cooling down engine intake both direct and indirect benefits are obtained. Some positive effects, as the improvement in volumetric efficiency are directly related with the reduction of intake air temperature. However, many of potential advantages are not directly related with this phenomenon so it is necessary to complete the study by readjusting fuel injection and combustion settings in the ICE according to the reduction in the intake temperature. Some of these potential advantages are listed below:

- A diminution in the NOx emissions associated to the reduction of peak temperatures during combustion due to the lower mean temperature of the flow (Cipollone et al., 2017).
- A reduction of thermal losses thus contributing to an adiabatic engine with higher indicated efficiency (Novella et al., 2017).
- Abnormal combustion (knocking effect) prevention in turbocharged gasoline engines

(Wang et al., 2017).

- Lower combustion temperatures associated to charge air cooling involving lower turbine inlet temperatures. As a result thermal stress is reduced.
- After treatment system or EGR line could be simplified since pollutant emissions are reduced.

In the present paper ejection cycle performance is modelled by means of a 1D model. One-dimensional models involving both ejector component and the whole cycle are also common in literature (Alexis and Karayiannis, 2005; W. Chen et al., 2013; García Del Valle et al., 2012; Huang et al., 1999).

The vast amount of literature published about sorption systems contrasts with the scarce attention that has been paid to ejection cycles in this area. Feasibility of cooling down gasoline engine intake using a jet-ejector cycle which uses exhaust as an energy source has been studied before by Zegenhagen and Ziegler (Zegenhagen and Ziegler, 2015a), (Zegenhagen and Ziegler, 2015b) following an experimental approach. Cooling capacities attained ranged between 2.3 and 5.3 kW for the corresponding thermal level and mass flow available on each engine operating point. Charge air temperatures ranged between 270.8 and 284.8 K depending on boundary conditions with R134a as working fluid.

As a novelty, the present paper introduces a genetic algorithm to maximize ejection cycle cooling capacity. Furthermore, performance degradation in *off-design* operating conditions is quantified. Unlike other research works, real gas assumption is prescribed and thermodynamic properties of the selected refrigerant are used in both cycle calculations and ejector map obtained with CFD. Likewise, the simple model presented allows to use as boundary conditions data coming from a specific ICE characterized experimentally.

The main objective of this work is the thermodynamic optimization of an exhaust gas driven jet-ejection cycle working with R134a intended to cool down the intake line of a diesel engine. The main goal covers both *design* (adaptable ejector size) and *off-design* (fixed ejector size) analysis over different engine operating points. Once both approaches are evaluated a critical discussion is carried out to determine performance limiting factors and possible solutions to improve cycle performance.

2. Ejection cycle model definition

In the present paper, an ejection cycle optimization is performed for a certain set of engine operating points by using a 1D theoretical model and then cycle performance is examined in *off-design* conditions. Ejector component is modelled with ejector maps obtained from numerical simulations, thus allowing to calculate cycle performance with a particular ejector prototype. Moreover, real data coming from experimental engine tests are used as boundary conditions.

2.1 Theoretical model hypothesis

Jet ejection cycle under investigation follows the scheme depicted in Figure *1* with the corresponding P-h and T-s diagrams (Figure *2*). Calculation process is simplified considering the following assumptions:

- Thermodynamic state of R134a gas is determined using real gas model. Refrigerant R134a has been chosen due to its good thermodynamic performance and its extended use in refrigeration systems in automotive industry (García Del Valle et al., 2014; Zegenhagen and Ziegler, 2015b). However, refrigerants exceeding GWP values higher than 150 are prohibited in vehicles since 2011. Furthermore, recent regulations (F-Gas Regulation 517/2014 together with F-Gas Regulation 842/2006) establish usage limits in fluorinated greenhouse gases and the need of avoiding the use of such gases where there are safe and energy-efficient alternative technologies with no impact or a lower impact on the climate. Therefore, R134a refrigerant in automotive industry has been phased out. Mentioned refrigerant has been used is this paper as a model. Authors consider that conclusions obtained with R134a as working fluid could be extended to new generation refrigerants with lower ODP and GWP since thermodynamic properties of new substitutes may be comparable. This decision is sustained by research works carried out by Lee and Jung (Lee and Jung, 2012) and Vaghela (Vaghela, 2017). Both research papers confirmed that R1234yf (HFO new generation refrigerant) can be used as a long term environmentally friendly solution of R134a in automotive applications with minor modifications. In the existing literature (Reasor et al., 2010) it is also highlighted that R1234yf is an ideal replacement to R134a due to their similar thermodynamic properties.

- Engine intake and exhaust flows are considered as a uniform ideal gas with constant values of specific heat capacity, mass flow and temperature.

- Ejector walls are considered as adiabatic (Eames et al., 1995).

- Ejector double-choking mode is assumed as the only admissible mode.

- Thermodynamic state of corresponding expansions inside the ejector (2) and (8) have been estimated considering double-choking operating mode. Secondary flow expansion has been deemed as an isentropic process, with constant isentropic efficiency ($\eta_{sec} = 0.9$), until reaching sonic conditions. Some authors suggest that secondary flow expansion efficiency is not constant and should be calculated according to ejector operating conditions (Besagni et al., 2015; Haghparast et al., 2018; Varga et al., 2009). A constant isentropic efficiency has been assumed in the present study in order to simplify the calculation process and save computational cost. Furthermore, the experimental/computational correlations given in the available literature to model expansion efficiency do not match with the particular operating conditions of this problem and present working fluid. The assumption of constant isentropic efficiency for secondary flow expansion around $\eta_{sec} = 0.9$ is also frequent in literature (Fangtian and Yitai, 2011; Huang et al., 1999). Resulting pressure of the secondary flow expansion (2) has been considered equal to the corresponding value at (8) which is a common approach at literature (Huang et al., 1999), (W. Chen et al., 2013). For primary flow expansion at converging-diverging nozzle one-dimensional model with real gas effects has been used (Zegenhagen and Ziegler, 2015c). The decision of modelling thermodynamic states (2) and (8) despite the adiabatic assumption is based on evaluating if a hypothetical mixture of liquid and vapor appears.

- Pressure losses are neglected in both evaporators and condenser.

- Pump efficiency is assumed to be constant and pressure rise is modelled by introducing an isentropic efficiency.

- Expansion process at the valve is assumed to be isenthalpic.

- Upstream the evaporator (0) mixture of liquid and vapor as well as subcooled liquid are considered as valid states.

- Both subcritical and supercritical are considered as feasible heating processes at generator.

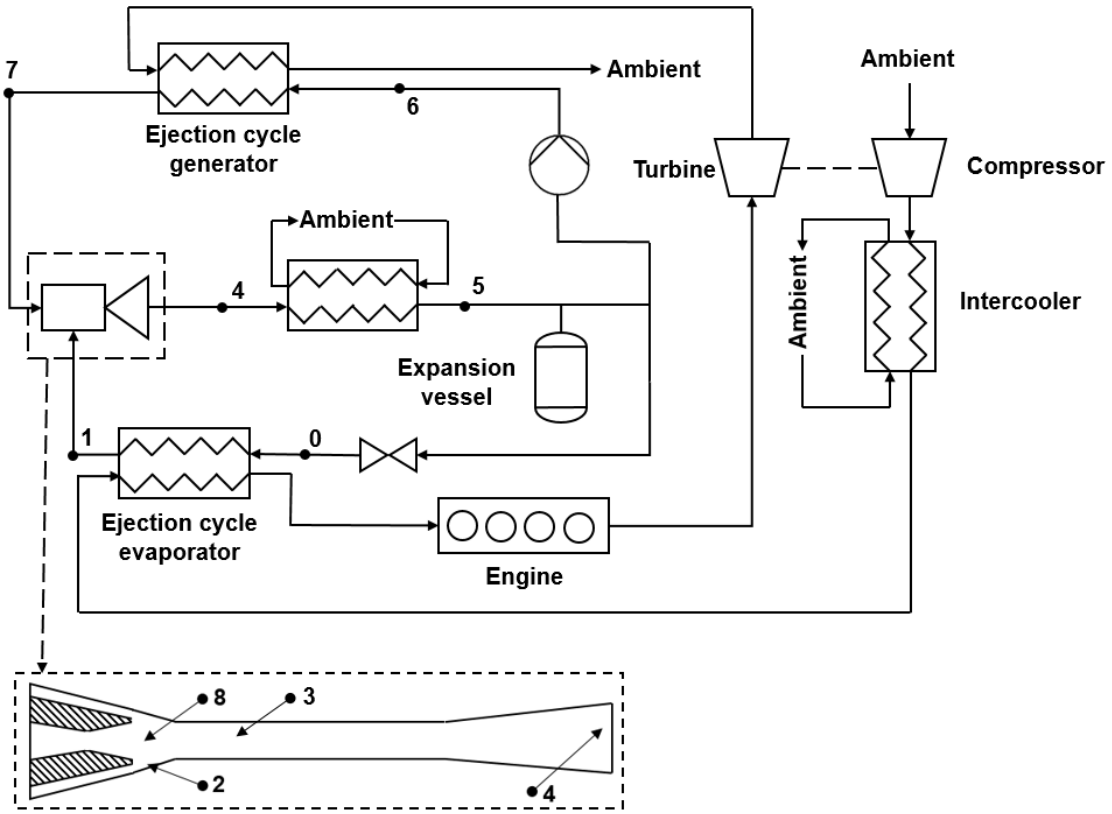

Figure 1. Ejection cycle arrangement intended to cool down engine intake

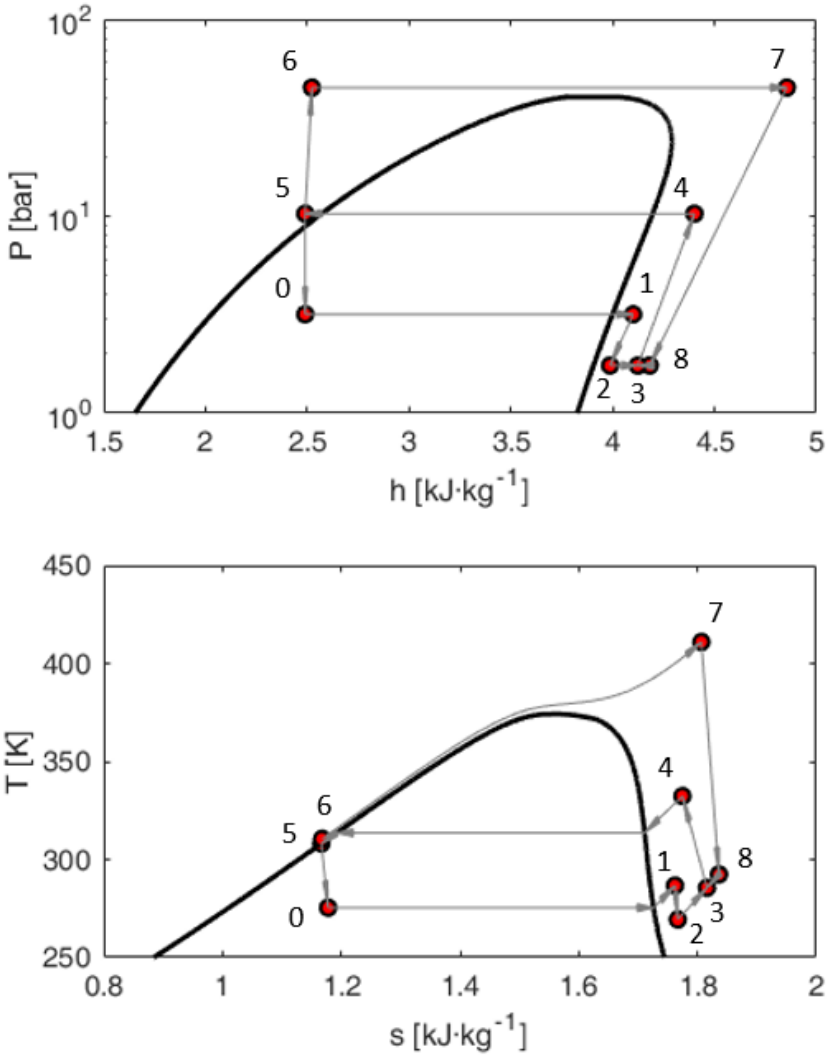

Figure 2. P-h and T-s diagrams of ejection cycle under investigation (R134a)

2.2 Cycle modelization

In this section ejector model is provided as well as equations to model thermodynamic state of both ejection cycle loops.

2.2.1 Ejector model

Ejector performance can be evaluated by means of characteristic surfaces which represent operating pressure ratios ($\pi_{1,7} = P_1/P_7$ and $\pi_{4,7} = P_4/P_7$) together with entrainment ratio ($\omega = \dot{m}_{sec}/\dot{m}_{pr}$) (Besagni et al., 2015; Zegenhagen and Ziegler, 2015b). Two characteristic modes are depicted in Figure *3*.

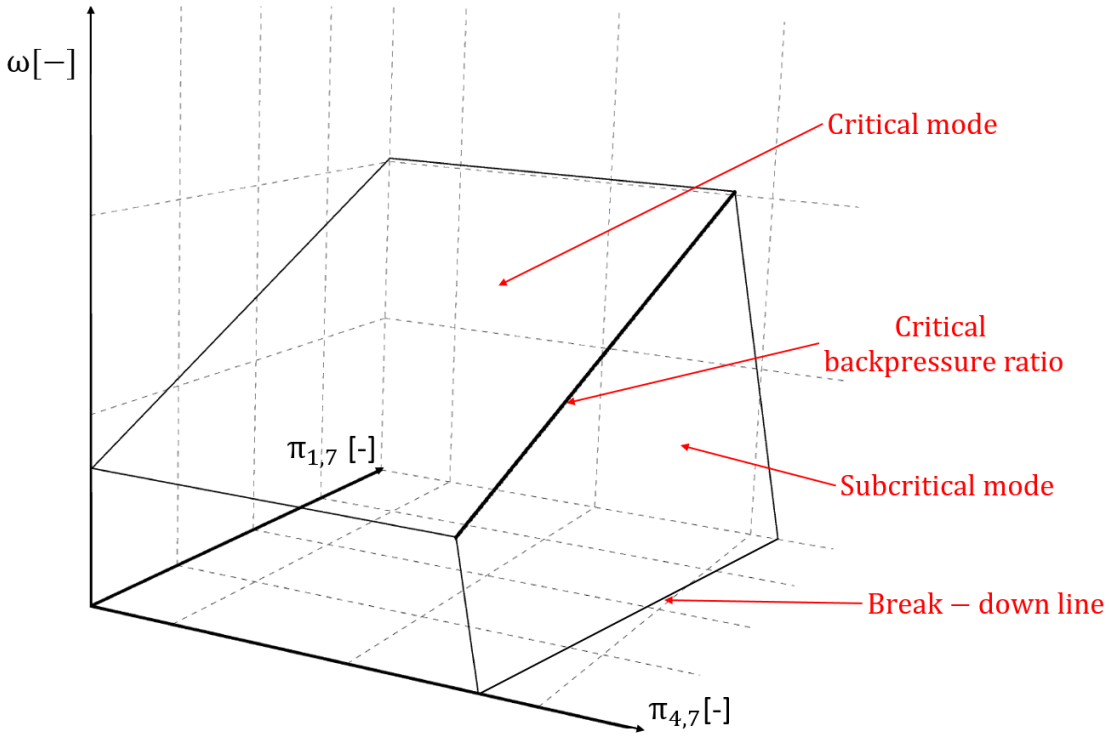

Figure 3. Ejector characteristic surfaces

According to Figure *3* two different modes can be distinguished: double-choking mode also called critical mode and single-choking mode, known as subcritical mode. In the present paper, simple expressions for ejector critical and subcritical maps for a single ejector prototype have been obtained numerically by means of CFD code and then introduced in the thermodynamic model to carry out cycle optimization. Backflow mode has been omitted because it does not have practical relevance.

2.2.2 Cycle operating pressures and mass flows

Starting from the assumption of negligible pressure loss at heat exchangers, inlet and outlet ejector pressure values can be determined with Equations (1), (2) and (3*)*.

$$P_4 = P_5 \tag{1}$$

$$P_0 = P_1 = P_5 - \Delta P_{vl} \tag{2}$$

$$P_6 = P_7 = P_5 \cdot k \tag{3}$$

Since the primary nozzle is operating in choking condition primary mass flow is determined following a real gas expansion model (Zegenhagen and Ziegler, 2015c). Thus, both the effect of primary flow pressure, temperature, thermodynamic behaviour of R134a and nozzle geometry are considered. Real gas effects are expected to be significant if primary flow pressure is high so this approach is appropriate.

$$\dot{m}_{pr} = \dot{m}_{pr}(A_{pr,t}, P_7, T_7, fluid, Z) \tag{4}$$

The secondary mass flow rate can be determined using entrainment ratio definition and ejector performance maps (Zegenhagen and Ziegler, 2015b) (Equations (*5*), (*6*) and (*7*)).

$$\dot{m}_{sec} = \dot{m}_{pr} \cdot \omega \tag{5}$$

$$\omega_{crit}(\pi_{1,7}, \pi_{4,7}) = \alpha_{1f} + \alpha_{2f} \cdot \pi_{1,7} + \alpha_{3f} \cdot \pi_{4,7} \tag{6}$$

$$\omega_{scrit}(\pi_{1,7}, \pi_{4,7}) = \alpha_{4f} + \alpha_{5f} \cdot \pi_{1,7} + \alpha_{6f} \cdot \pi_{4,7} \tag{7}$$

$$\omega(\pi_{1,7}, \pi_{4,7}) = \omega_{crit}(\pi_{1,7}, \pi_{4,7}) \quad if \quad \omega_{crit}(\pi_{1,7}, \pi_{4,7}) \leq \omega_{scrit}(\pi_{1,7}, \pi_{4,7}) \tag{8}$$

$$\omega(\pi_{1,7}, \pi_{4,7}) = \omega_{scrit}(\pi_{1,7}, \pi_{4,7}) \quad if \quad \omega_{crit}(\pi_{1,7}, \pi_{4,7}) > \omega_{scrit}(\pi_{1,7}, \pi_{4,7}) \tag{9}$$

2.2.3 Low pressure line

Flow conditions at evaporator inlet can be determined considering isenthalpic expansion at the valve:

$$h_5 = h(P_5, T_5) \tag{10}$$

$$h_0 = h_5 \tag{11}$$

$$T_0 = T(P_0, h_0) \tag{12}$$

Thermodynamic state of the flow at evaporator is obtained balancing heat exchanged at the engine and ejection cycle side:

$$\dot{Q}_{ev} = \dot{m}_{sec} \cdot (h_1 - h_0) = \dot{m}_{in} \cdot c_{p,in} \cdot (T_{i,in} - T_{o,in}) \tag{13}$$

Where h_1 can be calculated with a certain superheating temperature:

$$h_1 = h(P_1, T_1);\ T_1 = T_{v,sat} + T_{sup} \tag{14), (15}$$

$$T_{v,sat} = T(P_0, x = 1) \tag{16}$$

2.2.4 High pressure line

Thermodynamic state of the flow at generator inlet is obtained assuming isentropic pressure rise at the pump. Taking the thermodynamic state of (5) as starting point:

$$s_5 = s(T_5, P_5) \tag{17}$$

$$s_{6,s} = s_5;\ h_{6,s} = h(s_{6,s}, P_6) \tag{18), (19}$$

$$\eta_{pm} = \frac{h_{6,s} - h_5}{h_6 - h_5} \tag{20}$$

$$T_6 = T(h_6, P_6) \tag{21}$$

Where pump efficiency is assumed to be a given value $\eta_{pm} = 0.9$.

$$\dot{Q}_{ge} = \dot{m}_{ex} \cdot c_{p,ex} \cdot \left(T_{i,ex} - T_{o,ex}\right) = \dot{m}_{pr} \cdot (h_7 - h_6) \quad (22)$$

$$T_7 = T(h_7, P_7) \quad (23)$$

$$s_7 = s(T_7, P_7) \quad (24)$$

2.2.5 Middle pressure line

Phenomena of shockwave pattern has not been modelled over different operating conditions. Instead, adiabatic ejector hypothesis has been assumed:

$$\dot{m}_{pr} \cdot h_7 + \dot{m}_{sec} \cdot h_1 = \left(\dot{m}_{pr} + \dot{m}_{sec}\right) \cdot h_4 \quad (25)$$

$$T_4 = T(h_4, P_4) \quad (26)$$

Thermodynamic state downstream the condenser can alternatively be evaluated with conditions in (4). Introducing the energy conservation expression:

$$\dot{Q}_{co} = \dot{m}_w \cdot c_{p.w} \cdot \left(T_{o,w} - T_{i,w}\right) = \left(\dot{m}_{pr} + \dot{m}_{sec}\right) \cdot (h_4 - h_5) \quad (27)$$

The temperature downstream the condenser follows:

$$T_5 = T(h_5, P_5) \quad (28)$$

3. Ejection cycle optimization

This section presents the strategy followed to facilitate ejection cycle adaptation to *design* and *off-design* operating conditions as well as the genetic algorithm implementation for optimum search. Selection of design variables, boundary conditions and mechanical degrees of freedom is emphasized beside the constraints imposed to consider a particular point as feasible.

3.1 Ejector model

As mentioned before ejector component has been modelled by means of critical and subcritical characteristic surfaces. Primary nozzle exit diameter $(d_{n,o})$ and mixing chamber diameter (d_m) have been optimized with entrainment ratio by means of a parametric study carried out with CFD code using real gas model of R134a, while primary nozzle throat diameter is fixed as a constant value $(d_t = 1.8\, mm)$. Constant-pressure mixing ejector approach has been adopted, hence, primary nozzle exit is placed in the suction chamber. Experimental results available in literature (Zegenhagen and Ziegler, 2015b) have been used as reference boundary conditions for geometry optimization. Slight variations have been applied according to preliminary calculations with the present model and numerical stability criteria while solving CFD cases. With these assumptions ejector has been optimized considering primary flow pressure of 40 bar, secondary flow pressure of 4 bar and 13 bar of condenser backpressure. Primary nozzle exit

diameter ($d_{n,o}$) ranged from 2.4 mm to 3 mm in the parametric study whereas mixing chamber diameter (d_m) ranged from 3.1 mm to 3.7 mm. Optimum values have been found at 2.8 mm and 3.5 mm, respectively. Ejector dimensions under consideration guarantee a correct primary flow expansion and entrainment process. Hence, malfunctioning modes (backflow and recirculations) are avoided in the optimum geometry. Once optimum geometry has been determined ejector maps have been obtained by simulating different pressure boundary conditions with the fixed optimum geometry. For a fixed evaporating pressure, different condenser backpressure have been tested ranging from 11.2 bar to 14.4 bar. This procedure has been repeated for different evaporating pressures (ranging from 3 bar to 5.6 bar) until achieving a sufficient number of points to do an accurate fitting of both critical and subcritical modes depicted in Figure *3*. Resulting ejector maps are presented in Figure *4*.

All CFD cases under investigation have been simulated using a computational fluid dynamics code based on finite volume method. Three dimensional geometry of this particular problem has been taken into account by considering 2D domain with axisymmetry. Steady-state conditions and compressible turbulent flow are assumed since the flow inside the ejector is thought to be supersonic according to operating pressures. Inside the ejector single-phase hypothesis is also adopted. As the working fluid used in the ejector is R134a and the operating pressures are relatively high, the perfect gas assumption may not be an accurate approach (Zegenhagen and Ziegler, 2015c). For this reason real gas model has been adopted. Second order upwind spatial discretization schemes for turbulence and conservation equations have been selected and "Coupled" scheme for pressure-velocity coupling has been considered. Least Square Cell-Based is selected as gradient scheme and diffusion terms are discretized following second order central difference form. Pressure-based coupling model has been implemented according to satisfactory results reported in literature while modelling supersonic flow within ejectors (Croquer et al., 2016).

Reynolds Averaged Navier Stokes (RANS) approach has been employed in all simulations, and $SST\ k-\omega$ has been selected as turbulence model. There is good agreement with experimental data reported in the literature concerning supersonic flow within ejectors (Ruangtrakoon et al., 2013), (Zhu and Jiang, 2014), (Bartosiewicz et al., 2005), (Croquer et al., 2016; Kolář and Dvořák, 2011). Low-Reynolds approach has been followed, which has demonstrated to do an accurate description of flow phenomena in diffuser and mixing region. In these zones pressure gradients are significant due to the presence of shockwave pattern (Mazzelli and Milazzo, 2015). In primary nozzle, mixing zone and diffuser sections $y^+ < 1$ and low-Reynolds corrections have been enabled. A quadrilateral structured mesh (0.28E6 cells) with wall refinement is selected due to the prevalence of axial flow. Mesh independence is guaranteed since negligible variations in entrainment ratio (0.15%) are found when improving mesh refinement.

Previous numerical approach has been validated with jet-ejector experimental data available at the literature (García Del Valle et al., 2014). Discrepancies in entrainment ratio have been evaluated between the present CFD approach and ejector prototype "A" (García Del Valle et al., 2014) for seven operating conditions. Relative deviation in entrainment ratio between simulated and experimental data do not exceed 7.4%. Geometry and operating pressures of the ejector under investigation in the present study are comparable to those of the research work used for validation. Refrigerant used in both research works is also the same (R134a).

In order to create a simple model of ejector behaviour primary nozzle expansion model with real gas effects has been adopted. This hypothesis allows to introduce ejector scale by means of nozzle throat area (Equation (4)). Therefore, primary mass flow of the cycle can be altered by changing ejector scale.

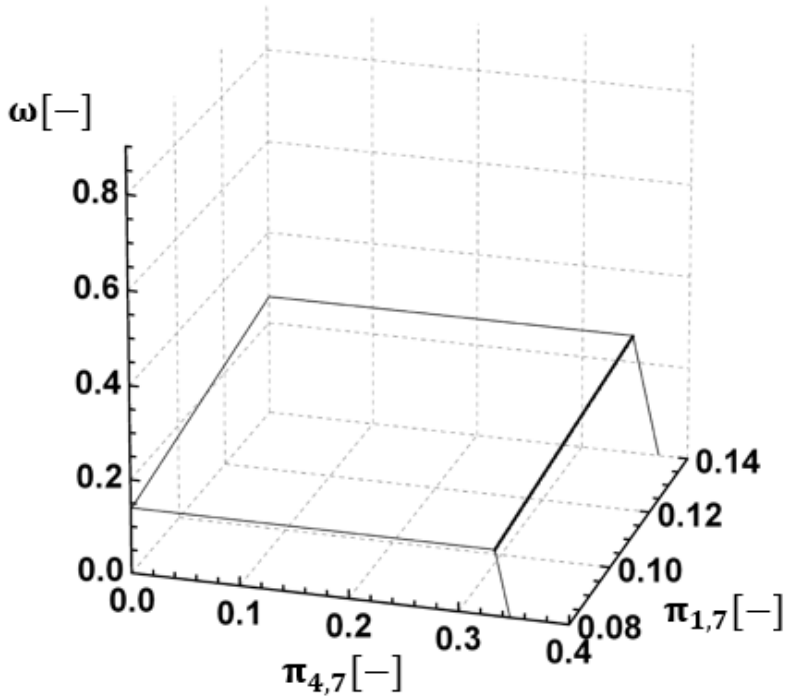

Figure 4. Ejector map optimized for $P_7 = 40\ bar$, $P_4 = 13\ bar$, $P_1 = 4\ bar$. Optimum dimensions correspond to $d_{n,o} = 2.8\ mm; d_m = 3.5\ mm$

3.2 Degrees of freedom

The control of the cycle is performed with a pump placed upstream the generator at the power loop and by using an expansion valve located downstream the condenser, as can be seen in Figure *1*. In addition, total available refrigerant is not a constraint and it can be controlled by introducing an expansion vessel. From these assumptions, pressure drop through the expansion valve (ΔP_{vl}), pump pressure ratio (k), and refrigerant total mass flow can be considered as degrees of freedom for the control loop.

3.3 Ejection cycle boundary conditions

Calculations are performed for a particular passenger car engine model characterized on an engine test bench. Analysed engine data come from a 1.5 l light duty diesel engine. Measured ICE intake/exhaust mass flow and temperature at each engine operating point are used as boundary conditions while carrying out ejection cycle optimization (Figure *5*). Mentioned parameters have been assessed with engine loads and speeds ranging from 25% -75% and 1500 rpm-3000 rpm, respectively. Resulting twelve engine operating points have been submitted to *design* and *off-design* study to analyse ejection cycle performance.

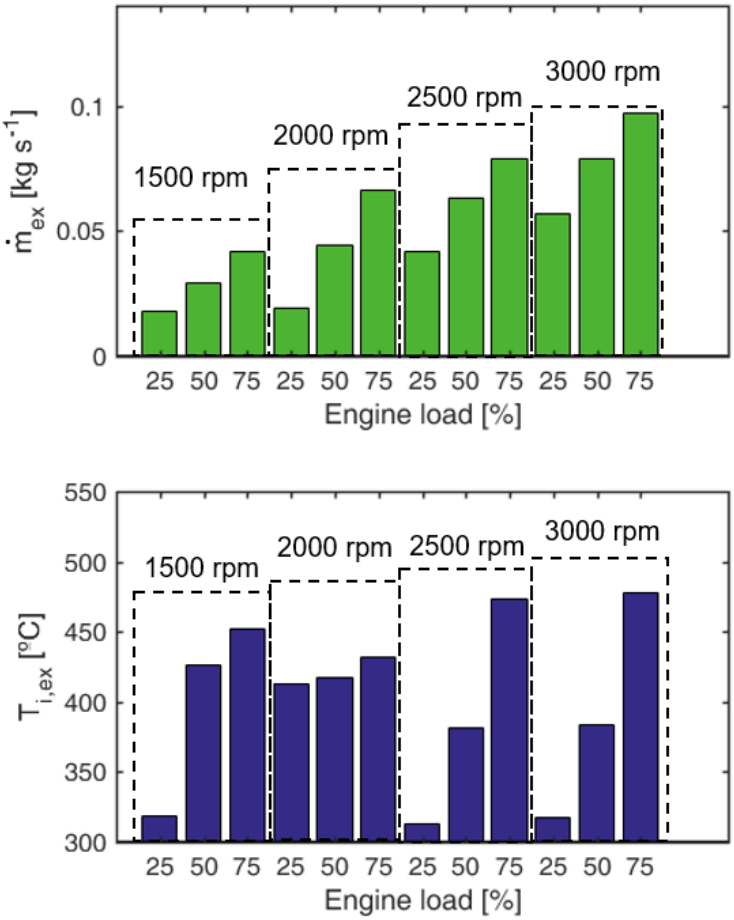

Figure 5. Exhaust temperature and mass flow over different engine operating points

In addition to engine operating conditions, specific heat capacity has been assumed for engine drawn air in hot and cold side, respectively. Furthermore, condenser temperatures on water side are assumed to be fixed values ($T_{i,w} = 30\ °C$, $T_{o,w} = 40\ °C$).

3.4 Model constraints

All simulated points must satisfy the following constraints to be considered as feasible:

- Only double-choking (critical) mode of Figure *3* has been considered as valid, however, single choking characteristic surface (subcritical mode) has also been determined at the definition of ejector map (Equation (7)) not as a feasible operating mode but as a limit to determine the boundaries of the double-choking surface.
- Enthalpy at (4) must be higher than vapor saturated enthalpy at condensing pressure to avoid liquid at ejector outlet.
- Enthalpy at (5) must be lower than liquid saturated enthalpy at condensing pressure to ensure 100% liquid at condenser outlet.
- Unstable system operation has been reported in literature due to the condensation effect on primary nozzle expansion (Grazzini et al., 2011). Hence, enthalpy at (2) and (8) must be higher than vapor saturated enthalpy at that pressure to avoid liquid inside the

ejector.

- Enthalpy at (7) must be higher than vapor saturated enthalpy at corresponding pressure to avoid liquid at ejector inlet. This condition is only applied below the critical point of the fluid.
- Evaporator superheating temperature must be greater or equal than zero.
- Pinch points during heat exchange process in both condenser, evaporator and generator must be greater than $10\ °C$ assuming counterflow heat exchangers.

3.5 Solution strategy in design and off-design conditions

Two significant studies have been conducted. The so-called *design* analysis regards adaptation to engine operating points presented on Figure *5* without restricting ejector size. Hence, this versatility allows to obtain relatively high performance over different conditions. In contrast, in *off-design* analysis a particular ejector size is selected according to the scaling factor that provided best results in *design* study for a single point. This point, set as 2000 rpm and 50% load of engine working conditions, has been designated because it is a frequent operating point in a standard driving behaviour. Therefore, *off-design* analysis restricts feasible points with a negative impact on overall cycle performance. General solving procedure of both cases is depicted in Figure *6*.

In addition to degrees of freedom indicated previously some thermodynamic variables have been varied during optimization process in order to improve the search of optimum values and not restrict valid operating points. Not all the mentioned variables of ejection cycle have been involved in *design* and *off-design* analysis because some of this variables are clearly delimited depending on the optimization case.

- Variables involved in *design* study are presented on Table *1*. Outlet exhaust temperature ($T_{o,ex}$) has remained constant since it has been proven that optimum value is precisely the admissible lower limit; 150 $°C$. This temperature has been limited to 150 $°C$ in order to avoid an excessive amount of combustion products in liquid phase.

Parameter	Lower limit	Upper limit
$\boldsymbol{\Delta P_v[bar]}$	7	14
$\boldsymbol{k}[-]$	3	4.5
$\boldsymbol{P_5[bar]}$	11	15
$\boldsymbol{T_{sup}[°C]}$	0	60
$\boldsymbol{\beta}[-]$	0.4	2.5

Table 1. Cycle variables modified during *design* analysis

- Variables involved in off-*design* study are presented on Table *2* with their corresponding bounds. As stated before, ejector geometry remains constant so the scaling factor (β) is fixed. However, temperature of exhaust gasses at generator outlet ($T_{o,ex}$) participates in the parametric study assuming that a hypothetical surplus of heat might exist.

Parameter	Lower limit	Upper limit
$\boldsymbol{\Delta P_v[bar]}$	7	14

$k[-]$	3	4.5
$P_5[bar]$	11	15
$T_{o,ex}[°C]$	150	475
$T_{sup}[°C]$	0	60

Table 2. Cycle variables modified during *off-design* analysis

In both *design* and *off-design* analysis T_5 has assumed to be equal to 40 $°C$ since it is the minimum admissible value to satisfy the corresponding pinch point at condenser.

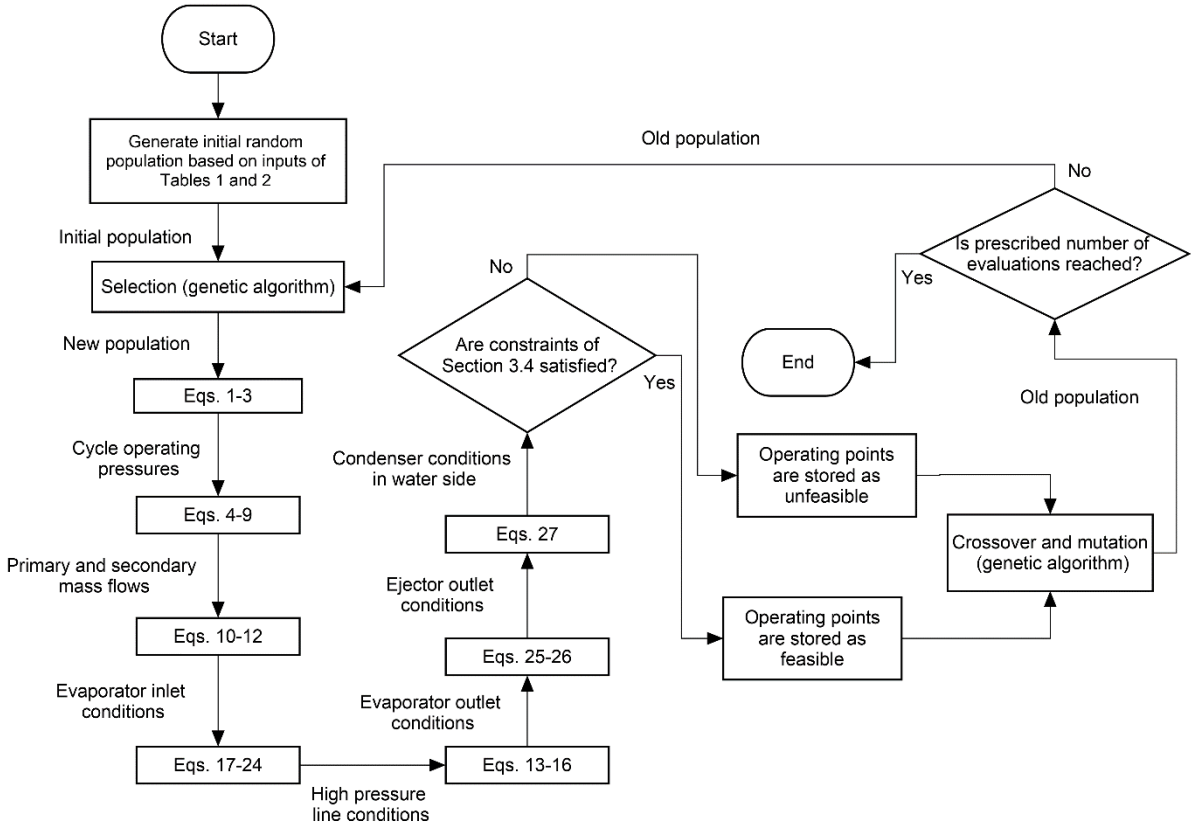

Figure 6. Flow diagram of the solving procedure

3.6 Genetic algorithm implementation

In the present analysis an ordinary parametric study is not feasible to find the best solution due to the high number of degrees of freedom involved. For this reason multi-objective genetic algorithm (MOGA-II) implemented in modeFrontier is employed. The input values are varied dynamically by modeFrontier over the specified ranges of the Table *1* and Table *2* allowing the optimization problem to evolve toward better solutions. Calculations are performed under mentioned constraints with a single objective: reduce intake air temperature ($T_{o,in}$) as much as possible.

4. Results and discussion

In this section, results in terms of cooling capacity (Q_{ev}) and engine intake outlet temperature ($T_{o,in}$) are provided in both *design* and *off-design* analysis.

4.1 Cycle performance in design conditions

Optimization has been performed for each engine operating condition described in Figure *5* (1500 rpm-3000 rpm and 25%-75% load). Parametric study with genetic algorithm MOGA II with variables shown in Table *1* and Table *2* has been implemented to find those feasible points with minimum intake air temperature. It must be noted that a reduction of engine intake temperature below $0°C$ has no practical interest and it would have a negative impact on engine performance due to intake line obstruction caused by ice formation. In the present study this operative limitation has not been exceeded. Intake temperature reduction is depicted on Figure *7*.

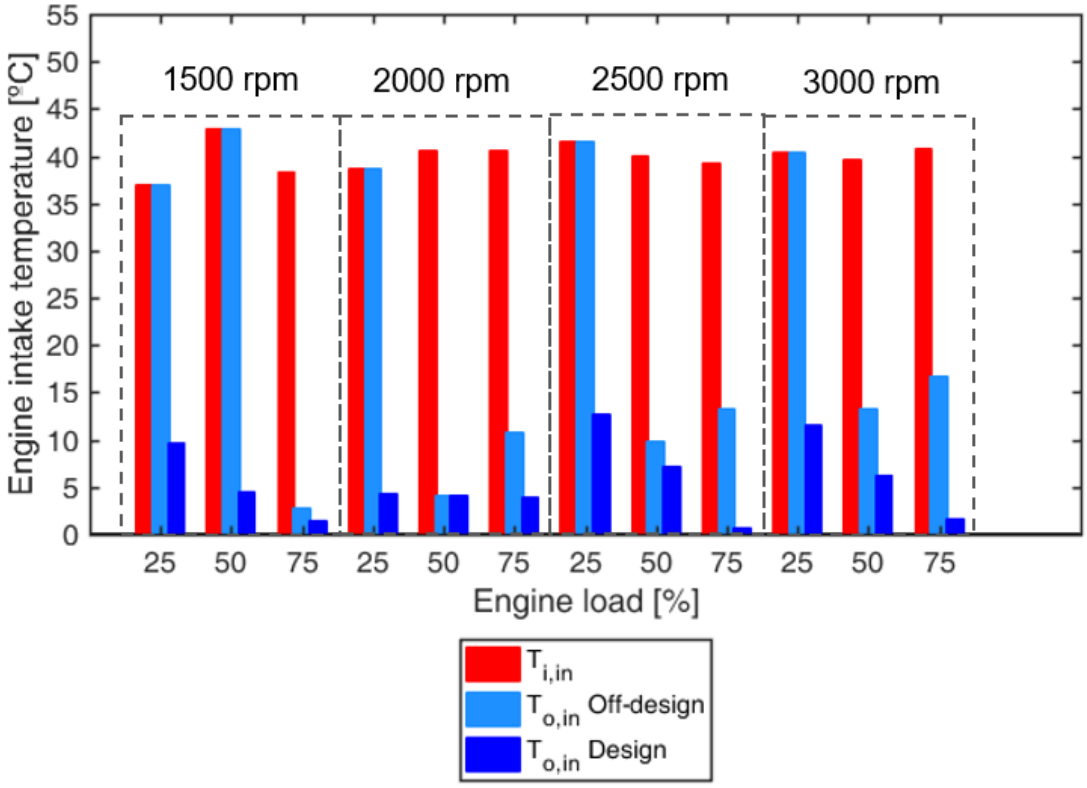

Figure 7. Engine intake temperature after cooling effect of ejection cycle in both *design* and *off-design* conditions

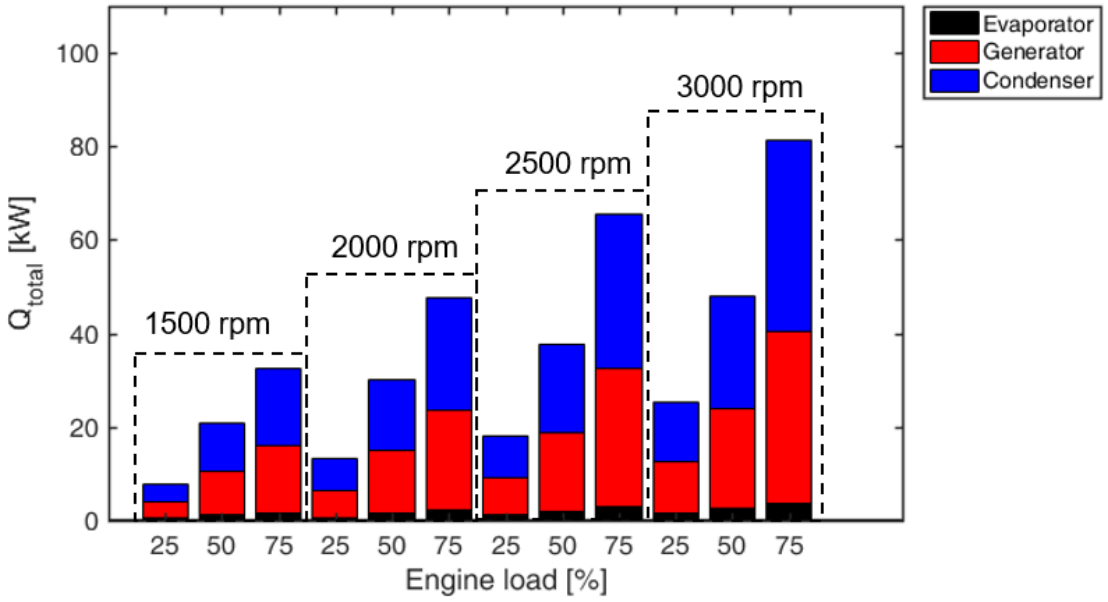

Figure 8. Condenser, generator and evaporator heat exchanged over different engine operating points in *design* study

Design results show that intake temperatures ranging between 0.7 °C and 12.7 °C can be attained with cooling capacities ranging from 0.46 kW to 3.66 kW. Those points with lower engine load are exceptions since thermal level at turbine outlet is not enough to obtain high performance at ejection cycle. Figure *8* depicts required cooling capacities of the cycle optimized for each engine operating point. As engine load and speed increases cooling capacities must increase accordingly to maintain best performance.

Over different engine loads and speeds required ejector scaling factor changes considerably, as can be reflected in Figure *9*, pointing out that numerous ejectors with different sizes would be required to obtain best performance in all operating points. Required ejector scaling factors range from 0.64 in the engine operating point with lower load and speed (25 % load and 1500 rpm) and 2.04 with higher load and speed (75 % load and 3000 rpm). Figure *9* depicts that an increase in engine load and speed results in a considerable increase of required ejector size. It should be noted that proposed scaling factors refer to size of the ejector simulated by means of CFD. Corresponding dimensions are described in section 3.1. With higher engine load or speed, mass flow aspirated by the engine ($\dot{m}_{in}$) and outlet turbine temperature ($T_{i,ex}$) increase. As a result, primary mass flow, must increase accordingly with the subsequent demand of larger ejector size. Over different operating points also equipment specifications differ significantly as can be seen in Figure *8*. For example, generator capacity with highest engine load and speed is almost triple the generator capacity of the reference operating point.

The coefficient of performance (COP), defined as ratio between cooling capacity and input power to cycle, i.e., ICE waste heat and power to drive the pump, show values ranging between 0.099 and 0.151. As a trend it can be observed that an increase in engine load leads to a decrease in COP. It can be attributed to an increase of thermal level and mass flow on engine exhaust. In such cases the rise in generator power is not accompanied by a proportional increase in cooling capacity.

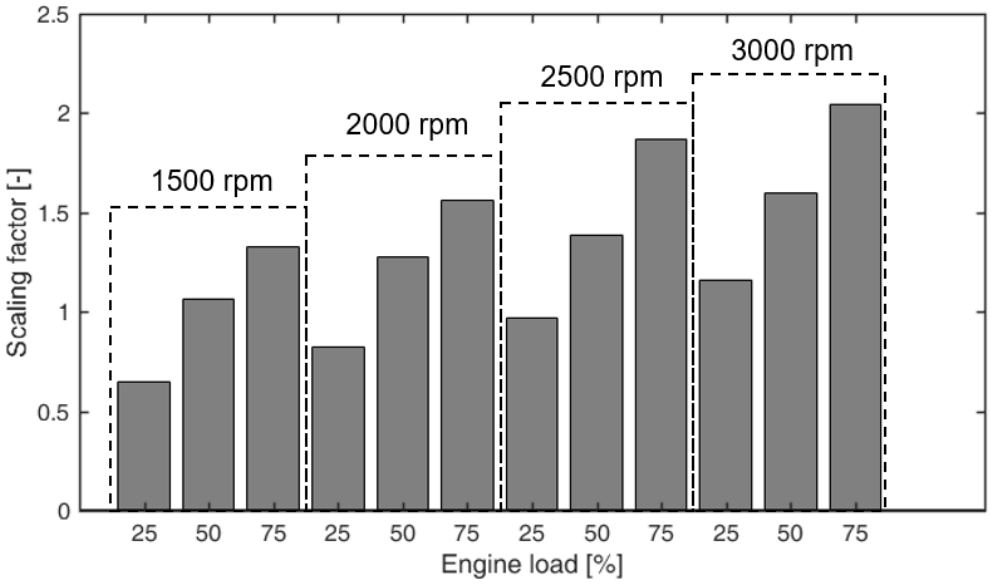

Figure 9. Required ejector scaling factor over different engine operating points

Throughout the simulations it has been observed that some constraints are increasingly limiting when temperature target is lower, so an upper bound to the heat transferred at evaporator arises. As mentioned previously, temperature at condenser outlet (T_5) is limited to a lower bound ($40\ °C$) to satisfy pinch point at condenser water side, so for a certain cooled intake air temperature (0°C as usual target) significant expansions are needed at the valve. This is because T_0 is required to be at least 10°C lower than cooled intake to satisfy the corresponding pinch point at evaporator. A low evaporation pressure (P_0) contributes to a low secondary-primary pressure ratio ($\pi_{1,7}$). According to ejector maps, lower $\pi_{1,7}$ means lower entrainment ratio and lower secondary mass flow with the corresponding reduction of heat transferred.

4.2 Cycle performance in off-design conditions

Once optimum ejector geometry has been obtained for each operating point the ejector scaling factor which provided best results for engine conditions of 2000 rpm and 50% load is selected. According to Figure *9* a scaling factor of 1.27 has been chosen. With this assumption performance of jet ejection cycle is examined in the rest of engine operating points.

Bar chart of Figure *10* illustrates how fixed ejector size limits power at heat exchangers with respect to the *design* study. Fixed ejector size affects the mass flow through power and refrigeration loops and therefore heat transferred at heat exchangers. This limitation becomes evident in those engine points with higher speed and load because mass flow at power loop is lower the required. For the engine point with 3000 rpm and 75% load heat exchanged at generator and evaporator is 58% and 38% lower with respect to the *design* analysis, respectively.

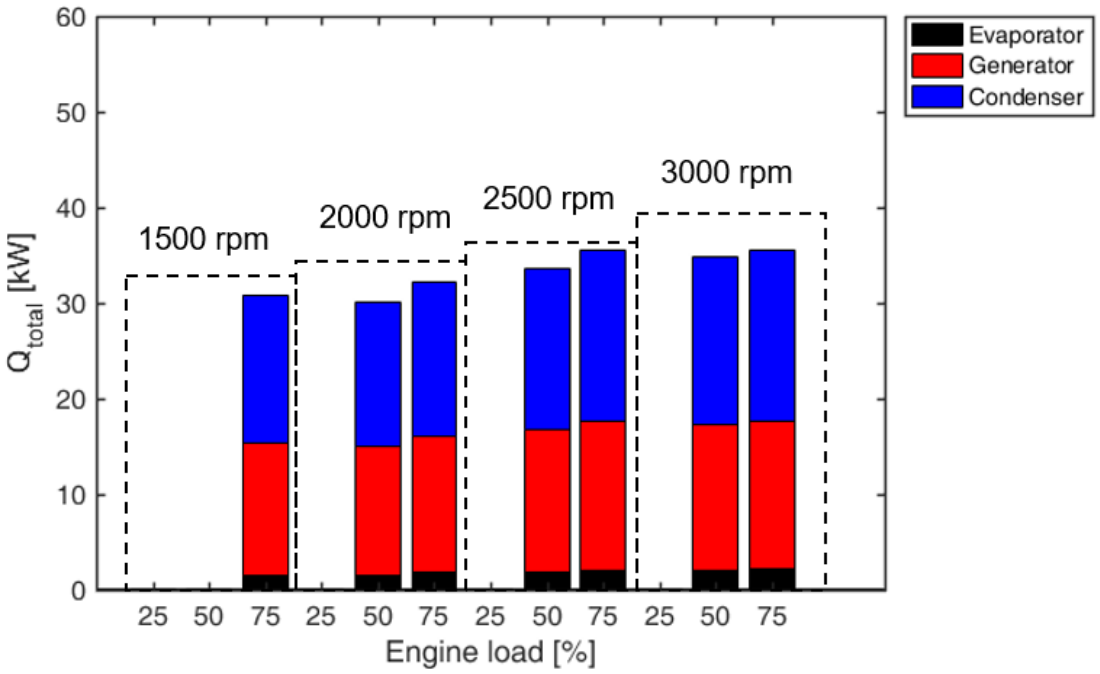

Figure 10. Condenser, generator and evaporator heat exchanged over different engine operating points in *off-design* study

As can be seen in Figure *11* the best performance is obtained for operating conditions comparable to the reference point. Those points which show similar intake/exhaust mass flow rates and temperatures show comparable performance, i.e, 75% load and 1500 rpm. Away from reference point, results are quite different since ejection cycle suffers a significant performance degradation. In *off-design* study minimum achievable temperatures range between 2.7 $°C$ and 16.7 $°C$. Figure *11* provides qualitative information about cycle performance and various regions can be distinguished. Temperature expressed as ΔT refers to the difference between *design* and *off-design* results:

- **Zone A:** There are no feasible solutions because thermal level of engine exhaust is not enough to avoid liquid at primary nozzle exit. Ejector is larger than the one required.
- **Zone B:** Poor solutions in terms of performance when compared to reference operating point are found. Secondary mass flow is far lower when compared to engine intake mass flow and cooling effect is less significant. Clearly, ejector size is smaller than the one required.
- **Zone C:** Solutions obtained are around the optimum values.

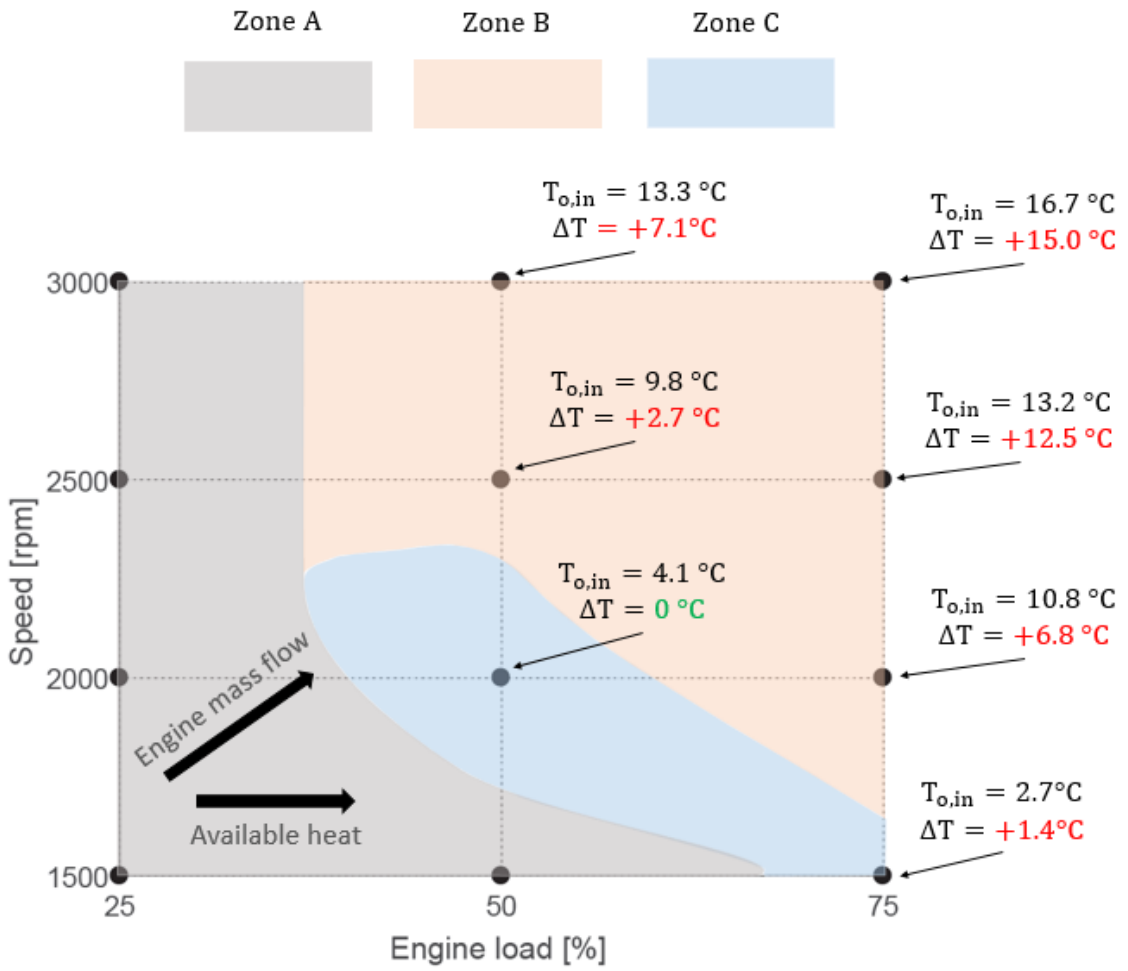

Figure 11. Ejection cycle performance degradation over different engine operating points

Almost fixed primary mass flow owing to the fixed ejector geometry is the most remarkable limiting factor during *off-design* optimum search. The limits of operating in *off-design* conditions with a certain ejector size and equipment can be understood taking into account ICE intake and outlet mass flows. In this particular problem both mass flows are almost identical with the only difference of fuel injected during combustion process. The cases stated below examine cycle performance with small ejector (low mass flow at power loop) and large ejector (high mass flow at power loop), respectively, with high and low thermal level in each case:

- **Mass flow at the power loop ($\dot{m}_{pr}$) is higher than mass flow through engine outlet ($\dot{m}_{ex}$):** This case is found generally when engine speed and load are lower than the reference operating point. If there is a low thermal level at engine exhaust then point (7) is close to vapor dome and liquid appears in (8) due to the subsequent expansion. Depending on the case analysed might not even reach superheated vapor conditions, i.e the constraint of keeping $T_{o,ex}$ over 150 °C is a limiting factor. Those cases shown on Figure *10* and Figure *11* which have no results exhibit this problem and any feasible solution has been found. On the contrary, if high thermal level is available at engine outlet enough heat can be transferred but $T_{o,ex}$ is close to 150 °C due to the relatively high mass flow at the power loop.

- **Mass flow at the power loop ($\dot{m}_{pr}$) is lower than mass flow through engine outlet ($\dot{m}_{ex}$):** This situation occurs when engine load and speed are higher than the reference point. Under this circumstance only a fraction total of heat available at engine exhaust is transferred. The limiting factor is found at evaporator where a relatively lower mass flow ($\dot{m}_{sec}$) at refrigeration loop might not be enough to achieve a substantial reduction on intake temperature. Ejector design plays a fundamental role in this case since greater entrainment ratios for a certain condition would lead to an increase of secondary mass flow with the subsequent rise of heat transferred.

In view of current results it is an obvious fact that this technology provides desired performance in a narrow range. Additional strategies should be integrated to guarantee $T_{o,in}$ close to 0°C away from reference point. Compressor-based refrigeration systems may be useful to extend the operative range of the conventional ejection cycle. The same positive effect could be achieved with an ejector prototype with adaptable nozzle geometry in order to compensate the lack or excess of heat at engine exhaust. Alternatively, ejectors with different geometrical shapes could be placed in parallel layout to be switched depending on engine operating conditions.

Some improvements of the system could be introduced with the current layout only modifying features of existing components. The system could be upgraded focusing efforts on ejector performance improvement. Ultimately, entrainment ratio could be improved for typical operating pressures. Considering heat exchangers capacity of the present study penalty over vehicle implementation would be acceptable with typical volumetric and gravimetric power densities of air conditioning equipment.

A substantial reduction in charge air temperature could be achieved with the refrigeration system under investigation even operating in *off-design* conditions. The cooling effect associated to temperature reduction would have a direct impact over volumetric efficiency improvement because density of charge air is increased. It also would have indirect benefits on engine performance after readjusting injection and combustion parameters. In that context, the cooling effect would reduce peak combustion temperatures with subsequent reduction in pollutant generation (NOx reduction) and turbine thermal stress. Furthermore, peak temperature diminution would also contribute to a more adiabatic engine and, consequently, it would improve engine indicated efficiency. Real improvement potential over pollutant emission, shaft power and fuel consumption should be quantified on an engine test bench.

5. Conclusions

In the present paper, a jet ejection cooling cycle is coupled to a 1.5 l diesel engine in order to cool down engine intake air by using waste heat recovery from engine exhaust gasses. The following results have been obtained:

- Charge air temperatures ranging from 0.7 °C to 12.7 °C with corresponding cooling capacities ranging from 0.46 kW to 3.66 kW can be attained depending on engine

operating point if ejector size is given as a design variable. Lower cooling capacities correspond with those engine operating points with lower engine load.

- When ejector size is fixed (optimum size for 2000 rpm, 50% engine operating point) performance is only maintained in a narrow band of engine operating points and only those engine points showing similar thermal level and drawn mass flow to the reference point achieve comparable performance. By contrast, with lower engine load no feasible solutions are found and with higher load and speed degraded performance is attained. Charge air temperatures range in this case between 2.7 $°C$ and 16.7 $°C$.

- Adaptation to high variety of ICE operating points has not been possible since fixed ejector geometry is a limiting factor. Therefore, with the current approach system interest lies on an ICE to be extensively used in a particular operating point and its vicinity since in this region desired performance is attained. In this regard, further investigation would be required to find strategies focused on performance improvement away from design point (double stage systems, ejector with variable geometry, compressor aided systems…).

Acknowledgements

Authors want to acknowledge to the institution “Conselleria d´Educació, Investigació, Cultura i Esport de la Generalitat Valenciana” and its grant program “Subvenciones para la contratación de personal investigador de carácter predoctoral” for doctoral studies (ACIF/2018/124).

Alexis, G.K., Karayiannis, E.K., 2005. A solar ejector cooling system using refrigerant R134a in the Athens area. Renew. Energy 30, 1457–1469. https://doi.org/10.1016/j.renene.2004.11.004

Bartosiewicz, Y., Aidoun, Z., Desevaux, P., Mercadier, Y., 2005. Numerical and experimental investigations on supersonic ejectors. Int. J. Heat Fluid Flow 26, 56–70. https://doi.org/10.1016/j.ijheatfluidflow.2004.07.003

Besagni, G., Mereu, R., Chiesa, P., Inzoli, F., 2015. An Integrated Lumped Parameter-CFD approach for off-design ejector performance evaluation. Energy Convers. Manag. 105, 697–715. https://doi.org/10.1016/j.enconman.2015.08.029

Chen, W., Liu, M., Chong, D., Yan, J., Little, A.B., Bartosiewicz, Y., 2013. A 1D model to predict ejector performance at critical and sub-critical operational regimes. Int. J. Refrig. 36, 1750–1761. https://doi.org/10.1016/J.IJREFRIG.2013.04.009

Chen, X., Worall, M., Omer, S., Su, Y., Riffat, S., 2013. Theoretical studies of a hybrid ejector CO2compression cooling system for vehicles and preliminary experimental investigations of an ejector cycle. Appl. Energy 102, 931–942. https://doi.org/10.1016/j.apenergy.2012.09.032

Cipollone, R., Di Battista, D., Vittorini, D., 2017. Experimental assessment of engine charge air cooling by a refrigeration unit. Energy Procedia 126, 1067–1074. https://doi.org/10.1016/j.egypro.2017.08.226

Croquer, S., Poncet, S., Aidoun, Z., 2016. Turbulence modeling of a single-phase R134a supersonic ejector. Part 1: Numerical benchmark. Int. J. Refrig. 61, 140–152. https://doi.org/10.1016/j.ijrefrig.2015.07.030

Diaconu, B.M., 2012. Energy analysis of a solar-assisted ejector cycle air conditioning system with low temperature thermal energy storage. Renew. Energy 37, 266–276. https://doi.org/10.1016/j.renene.2011.06.031

Eames, I.W., Aphornratana, S., Haider, H., 1995. A theoretical and experimental study of a small-scale steam jet refrigerator. Int. J. Refrig. 18, 378–386. https://doi.org/10.1016/0140-7007(95)98160-M

Fangtian, S., Yitai, M., 2011. Thermodynamic analysis of transcritical CO2refrigeration cycle with an ejector. Appl. Therm. Eng. 31, 1184–1189. https://doi.org/10.1016/j.applthermaleng.2010.12.018

García Del Valle, J., Sáiz Jabardo, J.M., Castro Ruiz, F., San José Alonso, J., 2012. A one dimensional model for the determination of an ejector entrainment ratio. Int. J. Refrig. 35, 772–784. https://doi.org/10.1016/j.ijrefrig.2011.11.020

García Del Valle, J., Saíz Jabardo, J.M., Castro Ruiz, F., San José Alonso, J.F., 2014. An experimental investigation of a R-134a ejector refrigeration system. Int. J. Refrig. 46, 105–113. https://doi.org/10.1016/j.ijrefrig.2014.05.028

Grazzini, G., Milazzo, A., Piazzini, S., 2011. Prediction of condensation in steam ejector for a refrigeration system. Int. J. Refrig. 34, 1641–1648. https://doi.org/10.1016/j.ijrefrig.2010.09.018

Gullo, P., Tsamos, K., Hafner, A., Ge, Y., Tassou, S.A., 2017. State-of-the-art technologies for transcritical R744 refrigeration systems - A theoretical assessment of energy advantages for European food retail industry. Energy Procedia 123, 46–53. https://doi.org/10.1016/j.egypro.2017.07.283

Guo, J., Shen, H.G., 2009. Modeling solar-driven ejector refrigeration system offering air conditioning for office buildings. Energy Build. 41, 175–181. https://doi.org/10.1016/j.enbuild.2008.07.016

Hafner, A., Banasiak, K., 2016. R744 ejector technology future perspectives. J. Phys. Conf. Ser. 745. https://doi.org/10.1088/1742-6596/745/3/032157

Haghparast, P., Sorin, M. V., Nesreddine, H., 2018. Effects of component polytropic efficiencies on the dimensions of monophasic ejectors. Energy Convers. Manag. 162, 251–263. https://doi.org/10.1016/j.enconman.2018.02.047

Huang, B.J., Chang, J.M., Wang, C.P., Petrenko, V.A., 1999. A 1-D analysis of ejector performance. Int. J. Refrig. 22, 354–364. https://doi.org/10.1016/S0140-7007(99)00004-3

Jiangzhou, S., Wang, R.Z., Lu, Y.Z., Xu, Y.X., Wu, J.Y., Li, Z.H., 2003. Locomotive driver cabin adsorption air-conditioner. Renew. Energy 28, 1659–1670. https://doi.org/10.1016/S0960-1481(03)00007-7

Koehler, J., Tegethoff, W.J., Westphalen, D., Sonnekalb, M., 1997. Absorption refrigeration system for mobile applications utilizing exhaust qases. Heat Mass Transf. und Stoffuebertragung 32, 333–340. https://doi.org/10.1007/s002310050130

Kolář, J., Dvořák, V., 2011. Verification of K-ω SST Turbulence Model for Supersonic Internal Flows. Waset.Org 5, 262–266.

Lee, Y., Jung, D., 2012. A brief performance comparison of R1234yf and R134a in a bench tester for automobile applications. Appl. Therm. Eng. 35, 240–242. https://doi.org/10.1016/j.applthermaleng.2011.09.004

Manzela, A.A., Hanriot, S.M., Cabezas-Gómez, L., Sodré, J.R., 2010. Using engine exhaust gas as energy source for an absorption refrigeration system. Appl. Energy 87, 1141–1148. https://doi.org/10.1016/j.apenergy.2009.07.018

Mazzelli, F., Milazzo, A., 2015. Performance analysis of a supersonic ejector cycle working with R245fa. Int. J. Refrig. 49, 79–92. https://doi.org/10.1016/j.ijrefrig.2014.09.020

Meunier, F., 2001. Adsorptive cooling: a clean technology. Clean Prod. Process. 3, 0008-0020. https://doi.org/10.1007/s100980000096

Novella, R., Dolz, V., Martín, J., Royo-Pascual, L., 2017. Thermodynamic analysis of an absorption refrigeration system used to cool down the intake air in an Internal Combustion Engine. Appl. Therm. Eng. 111, 257–270. https://doi.org/10.1016/j.applthermaleng.2016.09.084

Reasor, P., Aute, V., Radermacher, R., 2010. Refrigerant R1234yf Performance Comparison Investigation. Int. Refrig. Air Cond. Conf. Purdue 1–7.

Ruangtrakoon, N., Thongtip, T., Aphornratana, S., Sriveerakul, T., 2013. CFD simulation on the effect of primary nozzle geometries for a steam ejector in refrigeration cycle. Int. J. Therm. Sci. 63, 133–145. https://doi.org/10.1016/j.ijthermalsci.2012.07.009

Takeuchi, H., 2011a. Ejector with throttle controllable nozzle and ejector cycle using the same. Patent No. US 6,966,199 B2. https://doi.org/10.1016/j.(73)

Takeuchi, H., 2011b. Ejector cycle system. Patent No. US 6,729,149 B2. https://doi.org/10.1016/j.(73)

Talom, H.L., Beyene, A., 2009. Heat recovery from automotive engine. Appl. Therm. Eng. 29, 439–444. https://doi.org/10.1016/j.applthermaleng.2008.03.021

Tassou, S.A., Lewis, J.S., Ge, Y.T., Hadawey, A., Chaer, I., 2010. A review of emerging technologies for food refrigeration applications. Appl. Therm. Eng. 30, 263–276. https://doi.org/10.1016/j.applthermaleng.2009.09.001

Vaghela, J.K., 2017. Comparative Evaluation of an Automobile Air - Conditioning System Using R134a and Its Alternative Refrigerants. Energy Procedia 109, 153–160. https://doi.org/10.1016/j.egypro.2017.03.083

Varga, S., Oliveira, A.C., Diaconu, B., 2009. Numerical assessment of steam ejector efficiencies using CFD. Int. J. Refrig. 32, 1203–1211. https://doi.org/10.1016/j.ijrefrig.2009.01.007

Wang, Z., Liu, H., Reitz, R.D., 2017. Knocking combustion in spark-ignition engines. Prog. Energy Combust. Sci. 61, 78–112. https://doi.org/10.1016/j.pecs.2017.03.004

Zegenhagen, M.T., Ziegler, F., 2015a. Feasibility analysis of an exhaust gas waste heat driven jet-ejector cooling system for charge air cooling of turbocharged gasoline engines. Appl. Energy 160, 221–230. https://doi.org/10.1016/j.apenergy.2015.09.057

Zegenhagen, M.T., Ziegler, F., 2015b. Experimental investigation of the characteristics of a jet-ejector and a jet-ejector cooling system operating with R134a as a refrigerant. Int. J. Refrig. 56, 173–185. https://doi.org/10.1016/j.ijrefrig.2015.01.001

Zegenhagen, M.T., Ziegler, F., 2015c. A one-dimensional model of a jet-ejector in critical double choking operation with R134a as a refrigerant including real gas effects. Int. J. Refrig. 55, 72–84. https://doi.org/10.1016/j.ijrefrig.2015.03.013

Zhang, L.., 2000. Design and testing of an automobile waste heat adsorption cooling system.

Appl. Therm. Eng. 20, 103–114. https://doi.org/10.1016/S1359-4311(99)00009-5

Zhu, Y., Jiang, P., 2014. Experimental and numerical investigation of the effect of shock wave characteristics on the ejector performance. Int. J. Refrig. 40, 31–42. https://doi.org/10.1016/j.ijrefrig.2013.11.008